Modes of core–shell silver wire plasmonic nanolaser beyond Drude formula

2014 J. Opt. 16 075002

(http://iopscience.iop.org/2040-8986/16/7/075002)

IOP Publishing Journal of Optics
J. Opt. **16** (2014) 075002 (6pp) doi:10.1088/2040-8978/16/7/075002

Modes of core–shell silver wire plasmonic nanolaser beyond Drude formula

Denys M Natarov

Laboratory of Micro and Nano Optics, Institute of Radio-Physics and Electronics NASU, 61085 Kharkiv, Ukraine

E-mail: den.natarov@gmail.com

Received 1 April 2014, revised 14 May 2014
Accepted for publication 16 May 2014
Published 25 June 2014

Abstract

We consider the two-dimensional problem of a nonattenuating H-polarized electromagnetic field that can exist in the presence of a circular cylindrical nanowire (core) made of silver and coated with a concentric layer of active material (shell). Assuming that the natural-mode frequency is real-valued, we search for it together with the associated threshold value of material gain in the coating. Using the separation of variables, we arrive at a set of independent characteristic equations for each azimuthal index and seek their roots numerically. Here, it is important to use an adequate description of the metal core dielectric function. We observe that the well-known Drude formula not only leads to predictable errors in the lasing wavelengths but additionally, fails to reveal the complete composition of the modal spectrum. Known examples of sophisticated Drude-like formulas help overcome these drawbacks; however, these formulas suffer from negative absorption in silver in part of the visible range. Therefore, the use of experimental data for the metal dielectric function is mandatory. Our analysis reveals that, in each azimuthal order, the considered nanowire laser can emit light on several localized surface plasmon modes and the shell modes.

Keywords: nanolaser, nanowire, silver, lasing mode, localized surface plasmon

(Some figures may appear in colour only in the online journal)

1. Introduction

Recently, a true nanoscale laser has been demonstrated in a random ensemble of localized surface plasmon (LSP) mode assisted gold nanospheres coated with dye-doped silica shells [1]. In the article, it was suggested that the lasing occurred on the dipole-type LSP mode of the core–shell spherical nanocavity. Following this article, research began to appear that dealt with attempts of modeling core–shell spherical (in 3D) and circular cylindrical (in 2D) nanolasers [2–7]. These papers have reported certain useful results; however, they are not free from drawbacks. For instance, instead of studying source-free electromagnetic fields, research in [2–4] analyzes the scattering and absorption of a plane wave using an active scatterer. As a result, the conventional and fully adequate 'gain = loss' condition for the definition of threshold gain is erroneously replaced with the condition of a 'zero extinction cross section.' Research in [5–7] correctly deals with eigenvalue problems, assumes the presence of active regions, and extracts the lasing threshold gains from characteristic equations. More specifically, the work [5] studies the effect of adding a metal shell onto the thresholds of the whispering-gallery modes of an active core, but does not study the lasing on LSP modes. In [6], the dispersion of metal permittivity is neglected. Research in [7] addresses a specific approach, based on Finite-Difference Time-Domain simulations, that cannot handle eigenvalue problems in a direct manner (see discussion in [9]). Unlike these studies, our goal is the accurate consideration of a silver nanowire laser using the mathematically grounded lasing eigenvalue problem (LEP) approach, which has been earlier applied to several types of microcavity lasers [8–11].

2. Problem statement

The LEP approach is electromagnetic field eigenvalue problem tailored to provide both the modal frequencies and the

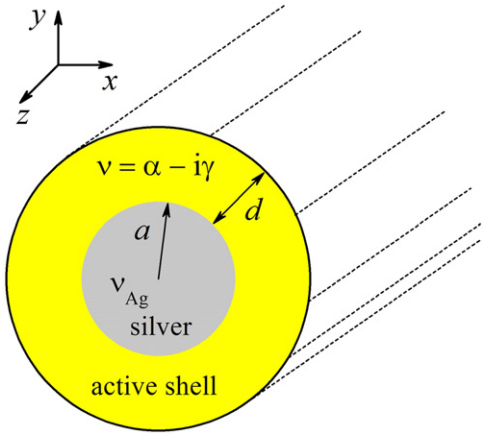

Figure 1. Nanowire laser as a core–shell open resonator with a concentric active region.

associated values of threshold material gain in the active region. It was first introduced in [8] and further generalized in [9], where the threshold gain has been explained via the overlap between the mode electric field and the active region. In the present paper, we extend these ideas to accurately determine the lasing thresholds and modal fields of an active shell nanowire laser.

Figure 1 shows the nanowire laser model under consideration. We suppose that a noble-metal wire (core) of the radius a is characterized by the refractive index $\nu_{Ag} = \varepsilon_{Ag}^{1/2}$, in which ε_{Ag} is dielectric permittivity. This wire is covered concentrically with an active material layer (shell) of thickness d, characterized by a complex-valued refractive index $\nu = \alpha - i\gamma$, in which $\alpha > 0$ is the refractive index, $\gamma > 0$ is the bulk material gain, and vacuum is the host medium.

The electromagnetic field is assumed to have the time dependence $e^{-i\omega t}$ and does not depend on z; the free space wavenumber is $k = \omega/c = 2\pi/\lambda$, in which λ is the wavelength and c is the light velocity.

The function we are seeking is the H_z field component, which must satisfy the Helmholtz equation with the appropriate wavenumber inside each layer, the Sommerfeld radiation condition at infinity, the condition of local power finiteness, and the continuity of the tangential field components at all boundaries.

Following [8], we consider the problem as an eigenvalue problem and search for pairs of real-valued parameters (λ, γ). The first of them is the mode emission wavelength and the second is the threshold value of material gain necessary to achieve lasing. Note that the gain per unit length, often used in semi-classical laser studies, can be obtained as $g = k\gamma$.

As mentioned previously, the electromagnetic field function satisfies the Helmholtz equations with corresponding wavenumbers in each of three domains of the studied nanolaser: metal core, dielectric shell, and free space host medium (as shown in figure 1). Here, an important question arises about the adequate description of the dielectric permittivity of silver.

3. Characterization of dielectric function of silver

Silver is a noble metal, characterized by the complex-valued dielectric function $\varepsilon_{Ag}(\lambda)$ in the visible range. The most remarkable circumstance is that its real part is negative because of the dominant contribution of the free-electron gas in the visible light frequencies. As a result, the value of $\mathrm{Re}\,\varepsilon_{Ag}(\lambda)$ varies from 0 to −30 in the wavelength range between 200 and 800 nm. The experimental values of complex dielectric functions of noble metals measured at discrete wavelengths can be found in classical works [12, 13]. In computer simulations, such values are required at any arbitrary wavelength that can be obtained either using numerical interpolation or deriving approximate analytical formulas.

As for analytical description, the Drude theory of electron conduction has long been a widely used instrument for the description of permittivity of plasma-like materials. The conventional Drude formula has two fitting parameters: plasma frequency ω_p and relaxation time τ_D, which can be assumed to be shape-independent constants for all dimensions of a metal sample exceeding 3 nm [14]. According to [15], the best fit for the $\mathrm{Re}\,\varepsilon_{Ag}(\lambda)$ of silver is achieved with $\omega_p = 1.32 \cdot 10^{16} s^{-1}$ and $\tau_D = 1.45 \cdot 10^{-14} s$; however, it still yields significant error if $\lambda \leqslant 400$nm. This selection also provides reasonable approximation of $\mathrm{Im}\,\varepsilon_{Ag}(\lambda)$, if λ is between 350 and 650 nm; however, it fails completely for $\lambda \leqslant 300$nm (see figure 2). As a result, the use of the Drude formula shifts the predicted positions of the LSP mode resonances into the ultraviolet range for a silver nanowire in a medium with $\varepsilon_{host} > 0$. These resonances are known to cluster near the wavelength, satisfying the equation $\mathrm{Re}\,\varepsilon_{Ag}(\lambda) \approx -\mathrm{Re}\,\varepsilon_{host}$ (see the discussion following figure 3).

Therefore, with growing demand for accurate modeling of plasmonic effects, a search for more sophisticated analytical descriptions of dielectric functions of metals had begun. Two improved analytical models have been introduced in [16–18] with more adequate descriptions: Drude plus four Lorentzian-pole pairs (D + 4L) and Drude plus two critical points (D + 2CP). Wavelength dependences of real and imaginary parts of the silver permittivity in the 200–800 nm range are shown in figure 2, computed with these two analytical models, and with experimental data of [12] interpolated using Akima splines. One can see better agreement of the D + 2CP model with data from [12]. However, both the D + 2CP and D + 4L models have another serious defect that prevents them from being used in the analysis of lasing in the significant part of the visible range. Both models yield the negative imaginary part of ε_{Ag} in the wavelength range between 400 and 600 nm, which formally corresponds to the erroneous appearance of the gain in the bulk silver instead of the losses.

The experiments have also shown that the silver permittivity of nanoparticles is dependent on sample quality, sample smoothness, and boundary materials [19, 20]. In our calculations, we used experimental data from [12], which are considered most accurate and compatible with nanowires and nanostrips [20]. Note also, that if the size of a metal particle is

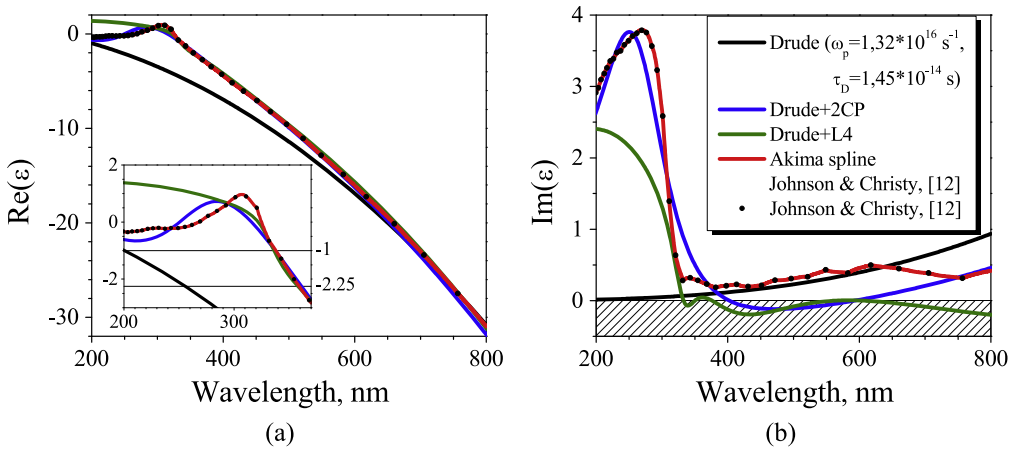

Figure 2. Real and imaginary parts of the silver permittivity as a function of the wavelength and a comparison of analytical and experimental data. The inset in panel (a) shows a zoomed-in image of the real part in the ultraviolet range.

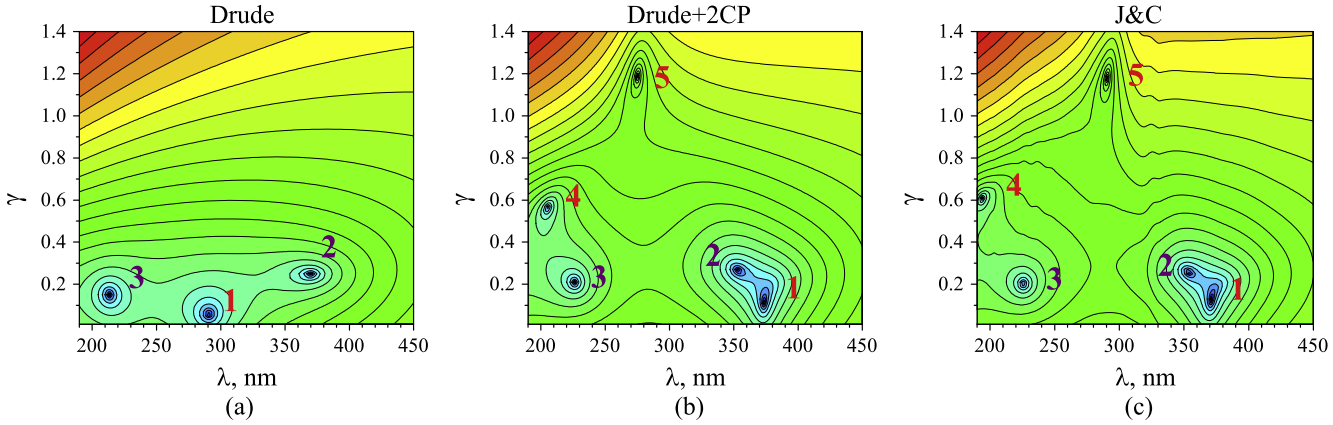

Figure 3. Reliefs of the absolute value of the left-hand part of the characteristic equation for a nanowire laser with $a = 30$ nm, $d = 170$ nm, $\alpha = 1.5$, and azimuth index $m = 2$. Dielectric function of silver is calculated using the Drude formula (a), D + 2CP method (b), and experimental data of [12] (c).

larger than 3 nm, all nonlocal effects can be neglected and the bulk values of the dielectric function can be used [14].

4. Analysis of lasing modes

Considering the electromagnetic field in the presence of our active shell nanolaser (figure 1), we note that the separation of variables, first introduced in 1881 by J. Strutt (later known as Lord Rayleigh) [21], leads to the splitting of the field function into separate azimuthal orders ($m = 0,1,2,\ldots$). This enables us to arrive at independent transcendental characteristic equations, $F_m(\lambda, \gamma) = 0$, for the modes of each order m and to study them separately (see also [22]). These equations contain the Bessel and Hankel functions of the arguments, depending on the refractive indices of all materials involved. Among the various roots of these equations: there are LSP mode eigenvalues whose wavelengths weakly depend on both the silver wire and the dielectric-shell radii. For a silver nanowire in free space, these modes cluster slightly in the red from the 350 nm wavelength. In the present work, we have investigated nanowire lasers with silver core radii from 20 to 100 nm, coated with active material in such a way that the total radius of layered structure is 200 nm. To determine the initial guess values, we calculated the relief of $\left|F_m(\lambda, \gamma)\right|$ as a function of γ and λ and searched for the minima of this function close to zero. Following this, a Newton-type iterative algorithm delivers the desired eigenvalue pairs with prescribed accuracy. We have searched for eigenvalues in the wavelength range of 190 to 700 nm and calculated them with the accuracy 10^{-8}.

The results presented next relate to the case of $m = 2$ (i.e., quadrupole modes), however the behavior of the eigenvalues in the other azimuthal families is quite similar. This is because of the well-known fact that the LSP modes exist for every m, except $m = 0$, and their wavelengths are given, in the leading term (i.e., neglecting the powers of $a/(a + d) < 1$ and $\gamma < 1$), by the root of the equation that does not depend on m, namely $\mathrm{Re}\,\varepsilon_{Ag}(\lambda) \approx -\alpha^2$ —see equation (10) of [22].

Figure 3 shows three reliefs of the function $|F_2(\lambda, \gamma)|$ corresponding to the silver core radius $a = 30$ nm, shell thickness $d = 170$ nm, and shell dielectric permittivity = 2.25 (i.e., the refractive index $\alpha = 1.5$ that corresponds to silica) in

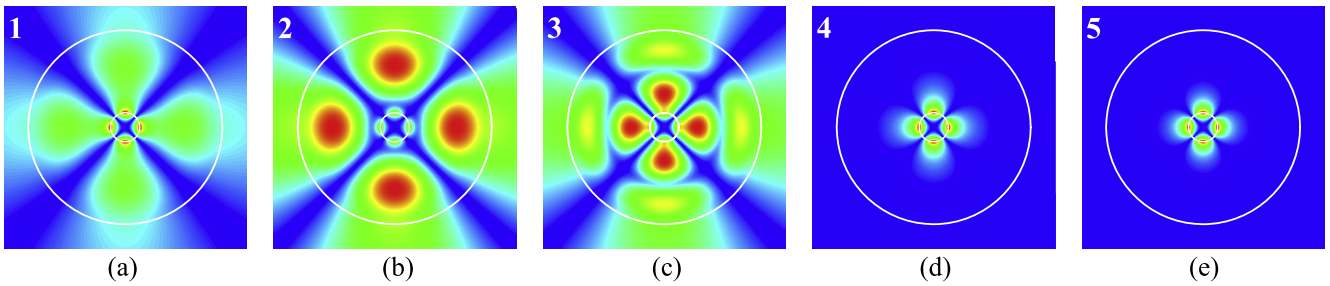

Figure 4. Near-field portraits for the H-polarized lasing modes of a nanowire laser computed using experimental data of [12] for the silver dielectric function. Numbers 1 through 5 correspond to the marks in panel (c) of figure 3. The associated lasing wavelengths and threshold values of material gain are $\lambda = 371.137$ nm and $\gamma = 0.128$ ($g \approx 21500$ cm^{-1}) for the principal LSP mode 1 (a), $\lambda = 353.440$ nm and $\gamma = 0.257$ for the first-order shell mode 2 (b), $\lambda = 225.737$ nm and $\gamma = 0.202$ for the second-order shell mode 3 (c), $\lambda = 193.922$ nm and $\gamma = 0.608$ for the secondary LSP mode 4 (d), and $\lambda = 290.491$ nm and $\gamma = 1.179$ for the secondary LSP mode 5 (e).

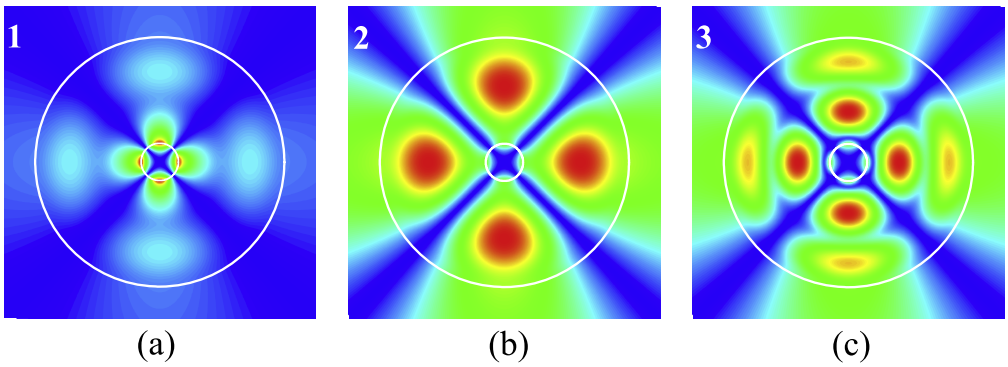

Figure 5. Near-field portraits for the H-polarized lasing modes of a nanowire laser computed using the Drude formula for the silver dielectric function. Numbers 1 through 3 correspond to the marks in panel (a) of figure 3. The associated lasing wavelengths and threshold values of material gain are $\lambda = 290.713$ nm and $\gamma = 0.058$ ($g \approx 12500$ cm^{-1}) for the principal LSP mode 1 (a), $\lambda = 370.001$ nm and $\gamma = 0.248$ for the first-order shell mode 2 (b), and $\lambda = 213.394$ nm and $\gamma = 0.150$ for the second-order shell mode 3 (c).

the strip of wavelengths between 190 and 450 nm. One relief has been computed using simple Drude formula with parameters from [15] (as on the corresponding curves shown in figure 2) for the silver permittivity [figure 2(a)], another has been computed using the improved formula D + 2CP from [16–18] (figure 2(b)], and the third has been computed using the experimental data from [12] [figure 2(c)].

Note that the relief computed with the aid of the D + 2CP model is very close to the relief based on the experimental data. This is because, in the considered range, this formula yields an accurate approximation of the experimental data (see figure 2).

The comparison reveals that, as expected, the simple Drude formula predicts the existence of the LSP mode (marked 1 in all three panels) however shifted, in wavelength, to violet approximately 80 nm from its true location [compare panels (a) and (c)]. The LSP lasing wavelength is slightly larger than the LSP resonance wavelength for a silver wire in free space because of the presence of a finite silica shell. This LSP mode has the lowest threshold value of material gain in the shell material. In addition to this mode, two other low-threshold modes exist in the same range of wavelengths (marked 2 and 3 in all three panels).

An unexpected result is that two additional higher-threshold modes exist that were not predicted by the simple Drude formula, but would be predicted if one uses the D + 2CP model. These higher-threshold nodes are marked as modes 4 and 5 in panels (b) and (c), respectively.

To classify and explain the nanowire laser modes, we analyzed the corresponding near-field patterns of the magnetic field $|H_z|$, normalized by its maximum value. This study has shown that modes 1, 4, and 5 are LSP-like modes (with the same azimuthal index $m = 2$). However, all these modes vanish if we use a nonplasmonic core material. Mode 1 can be called a principal quadrupole LSP mode and modes 4 and 5 can be called secondary quadrupole LSP modes of a circular silver wire. In contrast, modes 2 and 3 in panels (a)–(c) are the modes of the dielectric shell, slightly perturbed by the presence of the metal core. Near-field portraits that support this interpretation are shown in figure 4 for the five previously mentioned core–shell nanowire lasing modes from figure 3(c).

For comparison, the first three modes predicted by the Drude formula are also depicted in figure 5, based on the computations using the mentioned formula in the characterization of the silver dielectric function. As shown, the first- and second-order shell mode fields are visualized quite correctly, even when using the Drude formula for the metal core; however, the LSP mode field shows larger differences.

Note that within the adequate description of silver permittivity, the principal LSP mode (mode 1) and the first-order shell mode (mode 2) are close neighbors on the plane (λ, γ)

[figure 3(c)]. Because of this proximity, their field patterns show the features of hybrid modes, or supermodes, in the same manner as the modes of annular microcavities [23]. The near field of each displays the presence of the field spots that are characteristic to the other mode: the shell mode (mode 2) has a plasmon-like field pattern near the metal boundary, whereas the bright spots of the LSP mode (mode 1) extend far into the shell.

Concluding this analysis of lasing modes of an active shell circular silver nanowire, we note that each mode of any azimuth index $m>0$ is a double degenerate because of rotational symmetry. In practical situations, elementary core–shell nanoparticles can form random [1] or ordered [24] multiparticle configurations. If two or more circular nanowires equipped with active shells are brought together, this symmetry gets broken and degeneracy is removed, although the modes can form a close doublet.

5. Conclusions

In this paper, we have presented the results of an accurate analysis of the lasing wavelengths and material gain thresholds for a circular silver nanowire core coated with an active shell layer. Our study revealed that the simplified descriptions of the bulk silver dielectric function using the Drude formula, and its known sophistications, suffer from heavy inaccuracies that prevent them from being implemented into reliable analyses of lasing modes. The remedy is to use the experimental data supplemented with an appropriate smoothing interpolation.

With this approach, it is possible to see that both the LSP modes and the lower-order shell modes exist together in such a nanolaser. If the shell thickness is comparable to the emission wavelength scaled with the shell's refractive index, $\lambda\alpha$, then the LSP mode and shell mode lasing thresholds, in terms of material gain, can be comparable. To eliminate competition with the LSP mode, the shell thickness should be taken smaller, for instance, as a fraction of λ/α. In such a case, the shell modes are expected to shift to smaller wavelengths and obtain correspondingly higher thresholds because of the additional radiation losses.

Moreover, there is not one, but several, LSP-like modes, because of the complicated dispersion of silver; however, only one has a notably lower threshold and can be considered principal. These conclusions have been supported by the numerical data related to the quadrupole modes with the azimuthal index $m=2$; however, we expect similar results for the modes of the other indices.

Acknowledgments

This work was supported by the National Academy of Sciences of Ukraine via the State Target Program Nanotechnologies and Nanomaterials. Many fruitful discussions with E I Smotrova, A I Nosich, R Sauleau, and M Marciniak are appreciated and the valuable comments of two anonymous reviewers are acknowledged with gratitude.

References

[1] Noginov M A, Zhu G, Belgrave A M, Bakker R, Shalaev V M, Narimanov E E, Stout S, Herz E, Suteewong T and Wiesner U 2009 Demonstration of a spaser-based nanolaser *Nature* **460** 1110–2

[2] Pan J, Chen Z, Chen J, Zhan P, Tang C J and Wang Z L 2012 Low-threshold plasmonic lasing based on high-Q dipole void mode in a metallic nanoshell *Opt. Lett.* **37** 1181–3

[3] Baranov D G, Vinogradov A P, Lisyansky A A, Strelniker Y M and Bergman D J 2013 Magneto-optical spaser *Opt. Lett.* **38** 2002–4

[4] Ding P, He J, Wang J, Fan C, Cai G and Liang E 2013 Low-threshold surface plasmon amplification from a gain-assisted core–shell nanoparticle with broken symmetry *J. Opt.* **15** 105001

[5] Yao Q-F, Huang Y-Z, Zou L-X, Lv X-M, Lin J-D and Yang Y-D 2013 Analysis of mode coupling and threshold gain control for nanocircular resonators confined by isolation and metallic layers *J. Lightwave Techn.* **31** 786–92

[6] Tang L, Shi H, Gao H, Du J, Zhang Z, Dong X and Du C 2013 An eigenvalue method to study the threshold behaviors of plasmonic nano-lasers *Appl. Phys. B: Lasers and Optics* **113** 575–9

[7] Dridi M and Schatz G C 2013 Model for describing plasmon-enhanced lasers that combines rate equations with finite-difference time-domain *J. Opt. Soc. Am.* B **30** 2791–7

[8] Smotrova E I, Nosich A I, Benson T M and Sewell P 2005 Cold-cavity thresholds of microdisks with uniform and nonuniform gain: quasi-3D modeling with accurate 2D analysis *IEEE J. Sel. Top. Quant. Electron.* **11** 1135–42

[9] Smotrova E I, Byelobrov V O, Benson. T M, Ctyroký J, Sauleau R and Nosich A I 2011 Optical theorem helps understand thresholds of lasing in microcavities with active regions *IEEE J. Quant. Electron.* **47** 20–30

[10] Smotrova E I, Tsvirkun V, Gozhyk I, Lafargue C, Ulysse C, Lebental M and Nosich A I 2013 Spectra, thresholds and modal fields of a kite-shaped microcavity laser *J. Opt. Soc. Am.* B **40** 1732–42

[11] Smotrova E I and Nosich A I 2013 Optical coupling of an active microdisk to a passive one: effect on the lasing thresholds of the whispering-gallery supermodes *Opt. Lett.* **38** 2059–61

[12] Johnson P B and Christy R W 1972 Optical constants of the noble metals *Phys. Rev.* B **6** 4370–9

[13] Lynch D W and Hunter W R 1985 *In Handbook of Optical Constants of Solids* ed E D Palik (New York: Academic Press)

[14] Martin O J F 2003 Plasmon resonances in nanowires with non-regular cross-section *Optical Nano-Technologies, Topics Appl. Phys.* ed J Tominaga and D P Tsai (Berlin: Springer) pp 183–210

[15] Nash D J and Sambles J R 1996 Surface plasmon-polariton study of the optical dielectric function of silver *J. Mod. Opt.* **43** 81–91

[16] Vial A and Laroche T 2007 Description of dispersion properties of metals by means of the critical points model and application to the study of resonant structures using the FDTD method *J. Phys. D: Appl. Phys.* **40** 7152–8

[17] Vial A and Laroche T 2008 Comparison of gold and silver dispersion laws suitable for FDTD simulations *Appl. Phys.* B **93** 139–43

[18] Vial A, Laroche T, Dridi M and Le Cunff L 2011 A new model of dispersion for metals leading to a more accurate modeling of plasmonic structures using the FDTD method *Appl. Phys.* A **103** 849–53
[19] Hao F and Nordlander P 2007 Efficient dielectric function for FDTD simulation of the optical properties of silver and gold nanoparticles *Chem. Phys. Lett.* **446** 115–8
[20] Drachev V P, Chettiar U K, Kildishev A V, Yuan H-K, Cai W and Shalaev V M 2008 The Ag dielectric function in plasmonic metamaterials *Opt. Exp.* **16** 1186–95
[21] Strutt J W 1881 On the electromagnetic theory of light *Philos. Mag.* **12** 81–101
[22] She H-Y, Li L-W, Martin O J F and Mosig J R 2008 Surface polaritons of small coated cylinders illuminated by normal TM and TE plane waves *Opt. Exp.* **16** 1007–19
[23] Smotrova E I, Benson T M, Sewell P, Ctyroky J and Nosich A I 2008 Lasing frequencies and thresholds of the dipole-type supermodes in an active microdisk concentrically coupled with a passive microring *J. Opt. Soc. Am.* A **25** 2884–92
[24] Natarov D M, Sauleau R, Marciniak M and Nosich A I 2014 Effect of periodicity in the resonant scattering of light by finite sparse configurations of many silver nanowires *Plasmonics* **9** 389–407